

## IRWST

## An Experimental Study on the Direct Contact condensation of steam and Air bubble Oscillation in IRWST

KNGR IRWST  
 가 가 가  
 가 RMS  
 IRWST  
 가

### Abstract

We investigated and analyzed the direct contact condensation of steam and the oscillation of air bubble. And we characterized the pressure oscillation resulting from those. The experiment result showed as follows. In chugging region, the high pressure pulse generation rate was little affected by the subcooled water temperature but increased with increasing the steam mass flux. In the region of condensation oscillation and stable condensation, the variation of frequency of dynamic pressure was decreased with increasing of the water temperature. And decreased as increasing nozzle diameter. The amplitude of pressure oscillation was maximum at the boundary between these two region, and remarkably decreased in the stable condensation region. In the case of air bubble, showed that the frequency of air bubble oscillation decreased with increasing the quantity of injected air.

1.

IRWST

가  
가  
가  
가  
[1].

/  
가  
가  
IRWST  
가

## 2.

### 2.1

Fig. 1

가  
가  
2.2 (test section)  
Fig. 2

RTD  
가  
가 600 mm  
가  
8 mm  
8 mm, 30 mm  
30 mm  
overflow  
m<sup>3</sup>  
350 mm  
가 500 mm, 0.18

### 2.3

Table 1  
3/8, 4/8, 5/8, 6/8 inch 가  
3/8 inch  
4/8 inch

5/8, 6/8 inch  
 20 kg/m<sup>2</sup>sec 가 가  
 50 kg/m<sup>2</sup>sec  
 30~90

2.4

(Fig 3~5).  
 가 가

FFT  
 RMS(Root Mean Square)

$$RMS\ pressure = \frac{\sum_{i=1}^N \sqrt{(p_m - p_i)^2}}{N}$$

2.4.1

가  
 FFT 가 가

가 Fig. 6 6/8 inch 가 70 가  
 60 kg/m<sup>2</sup>sec 가  
 가 80 kg/m<sup>2</sup>sec 가  
 가 60~80 kg/m<sup>2</sup>sec 가 80

가 Fig. 7 가  
 80 kg/m<sup>2</sup>sec 60 kg/m<sup>2</sup>sec 가  
 가  
 ( G < 80 kg/m<sup>2</sup>sec)  
 가

10 kg/m<sup>2</sup>sec 10 Hz , 20~60 kg/m<sup>2</sup>sec 20~50 Hz  
 IRWST 30 Hz  
 가  
 3~7 Hz 가 [2]가

Fig. 8 /

가 가

Fig. 9  
가

가

### 2.4.2

-

Fig. 10 가 30, 40 가  
 350 kg/m<sup>2</sup>sec 가  
 300 kg/m<sup>2</sup>sec ,  
 [2][3]. 가  
 가 가  
 가 가  
 가 가  
 가 가  
 가 가  
 가 가

Fig. 12

가

RMS

300 kg/m<sup>2</sup>sec 가 RMS 가 Fig. 13  
 350 kg/m<sup>2</sup>sec 가  
 가 80  
 250 kg/m<sup>2</sup>sec 300 kg/m<sup>2</sup>sec,

### 3.

#### 3.1

Fig. 14

600 × 600 × 600mm  
 150 mm  
 300 mm hole 400 mm,  
 24 hole, 8 hole  
 (PT3,PT2) (pressure transducer)  
 (PT1)

#### 3.2

가  
 Table 2

가 가

1~7

가

0.05~0.3

3.3

hole

가

Fig. 15~16

Fig. 16

가

가  
가  
가

가

가  
[4].

Fig. 15

Fig. 16

0.2

0.5

Fig. 17~18

가

1bar

hole

가 가

가

가

가

가

4.

1)

가

가

가

2)

가

3)

가

4)

가

가

5)

가

가 IRWST 가 (  $G < 80 \text{ kg/m}^2\text{sec}$  )

가

KAERI , NRL

- [1] P. J. Kerney, G. M. Feath, and D. R. Olson, "Penetration Characteristics of a Submerged Steam Jet", AIChE J., Vol. 18, No. 3, pp. 548–553, 1972
- [2] S. Cho, C. H. song, C. K. Park, S. K. Yang, and M. K. Chung, "Experimental Study on Dynamic Pressure Pulse in Direct Contact Condensation of Steam Jets Discharging into Subcooled Water", NTHAS98, pp. 291–298, 1997
- [3] Y. S. Kim, "An Investigation of Direct Contact Condensation of Steam Jet in Subcooled Water", PhD. Dissertation, KAIST, 1996
- [4] S. Cho, S. K. Yang, H. J. Chung, S. Y. Chun, " Characteristics of Air Clearing Loads of a Sparger, Proc. of the Korean Nuclear Society Autumn Meeting, 2000
- [5] M. E. Simpson and C. K. Chan, "Hydrodynamics of a Subsonic Vapor Jet in Subcooled Liquid", J. of Heat Transfer, Vol. 104, pp. 271–278, 1982
- [6] I. Aya and H. Nariyai, "Evaluation of Heat-transfer Coefficient at Direct Contact Condensation of Cold Water and Steam", Nucl. Eng. and Des., Vol. 131, pp. 17–24, 1991
- [7] C. K. Chan. and C. K. B. Lee, "A Regime Map for Direct Contact Condensation", Int. J. Multiphase Flow. 8, No. 1, pp. 11–20, 1982

Inner diameter of nozzle	Mass flux (kg/m <sup>2</sup> sec)	Temperature(°C )
3/8 inch	20, 40, 60, 80, 100	30~90 °C
	120, 150, 200, 250, 300, 350, 400	
4/8 inch	20, 40, 60, 80, 100	30~90 °C
	120, 150, 200	
5/8 inch	20, 40, 60, 80, 100, 120	30~90 °C
6/8 inch	20, 40, 60, 80, 100	30~90 °C

Table 1. Experimental parameters and ranges (steam)

hole	(bar)	(sec)
8 hole	1, 3, 5, 7	0.05, 0.1, 0.2, 0.3
24 hole	1, 3, 5, 7	0.05, 0.1, 0.2, 0.3

Table 2. Experimental parameters and ranges (Air)

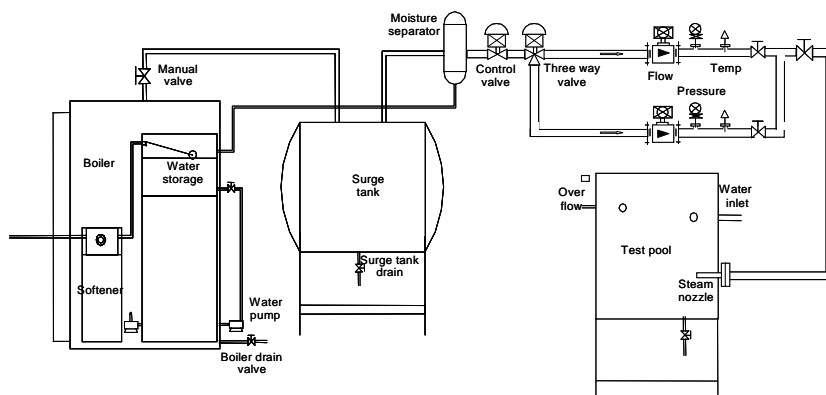


Fig.1 Schematic diagram of experimental facilities

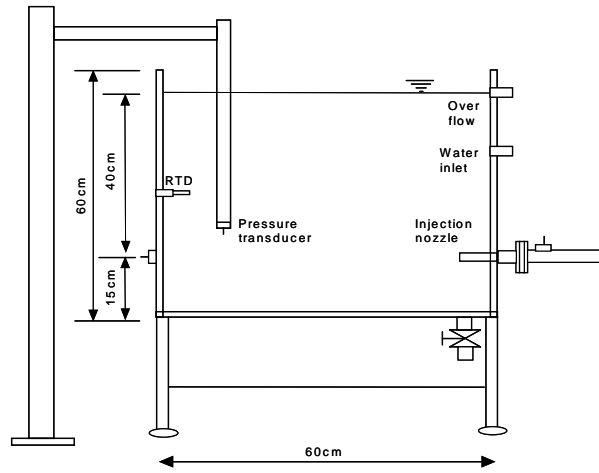


Fig.2 Schematic diagram of test section

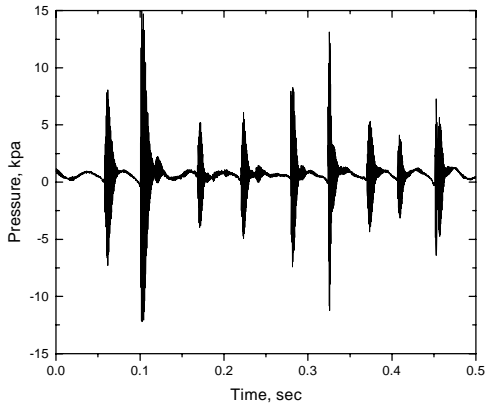


Fig.3 Chugging region  
( $G=20 \text{ kg/m}^2\text{sec}$ ,  $T=40^\circ\text{C}$ )

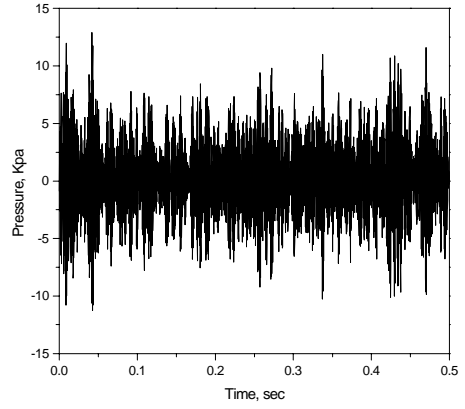


Fig.4 Condensation oscillation  
( $G=200 \text{ kg/m}^2\text{sec}$ ,  $T=40^\circ\text{C}$ )

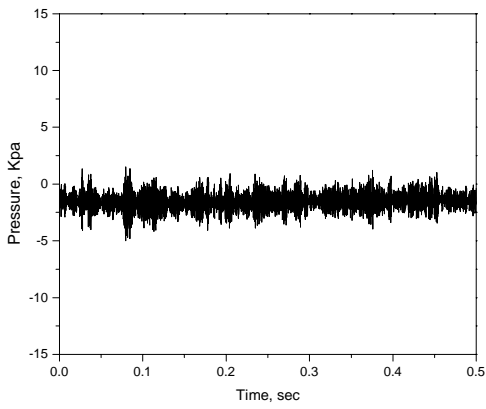


Fig5. Stable condensation  
( $G=200 \text{ kg/m}^2\text{sec}$ ,  $T=40^\circ\text{C}$ )



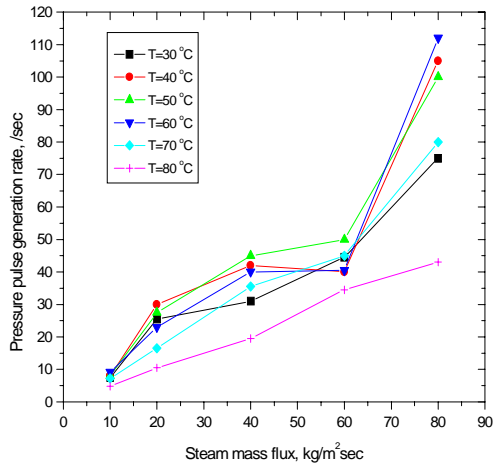


Fig.6 Pressure pulse generation rate with steam mass flux in chugging region (d=6/8 inch)

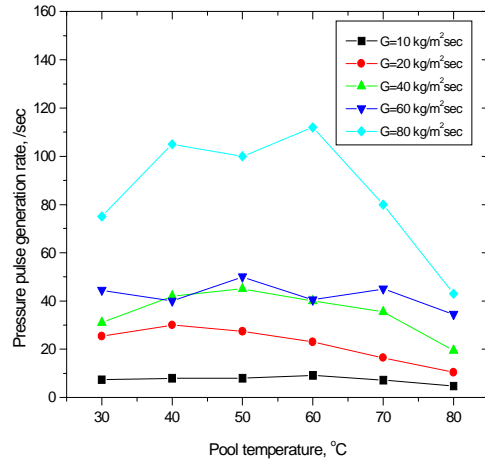


Fig.7 Pressure pulse generation rate with pool temperature in chugging region (d=6/8 inch)

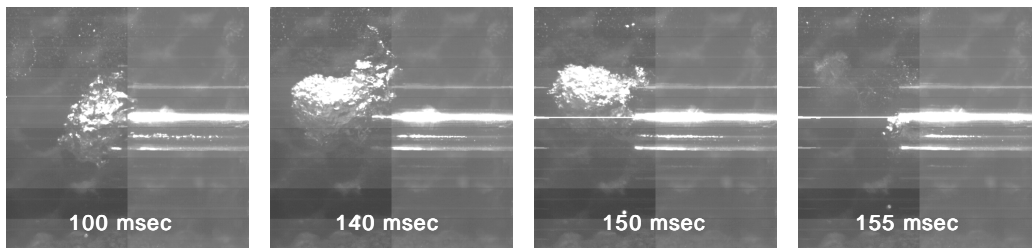


Fig.8 Time history interface variaton with necking phenomenon

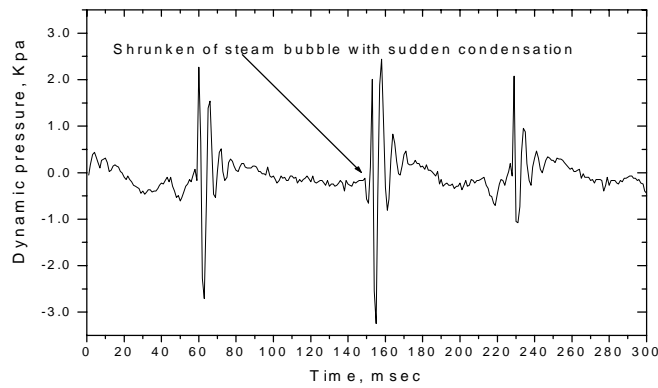


Fig.9 Time history of pressure with interface variaton

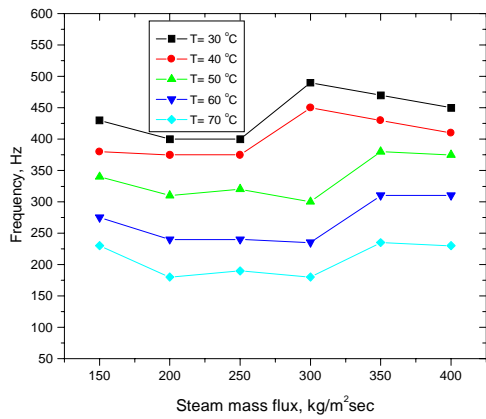


Fig.10 Frequency variation with Steam mass flux (d=3/8 inch)

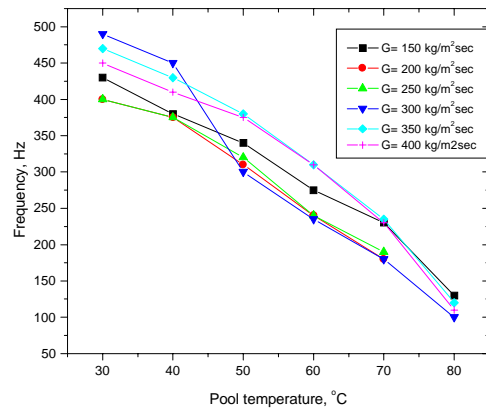


Fig. 11 Frequency variation with pool temperature (d=3/8 inch)

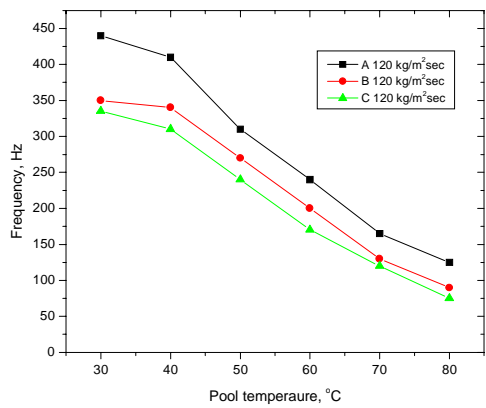


Fig.12 Frequency variation with nozzle diameter (A: 3/8inch B: 4/8inch C:6/8inch)

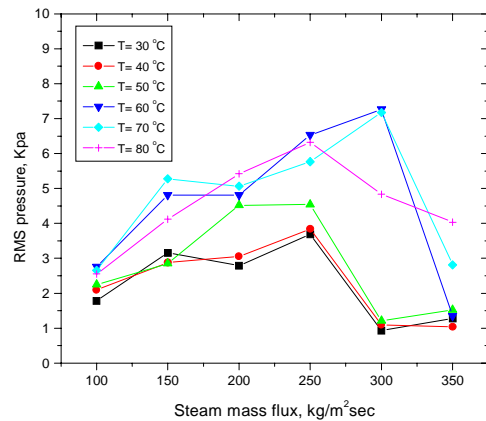


Fig.13 Frequency variation with steam mass flux (3/8 inch)

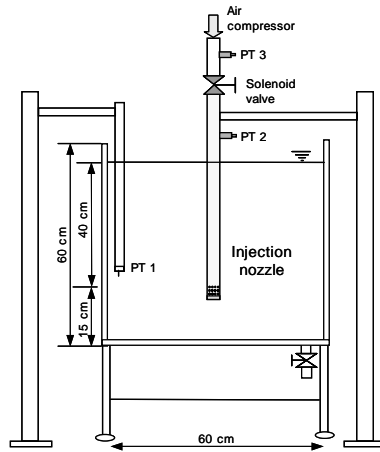


Fig. 14 Schematic diagram of experimental facilities

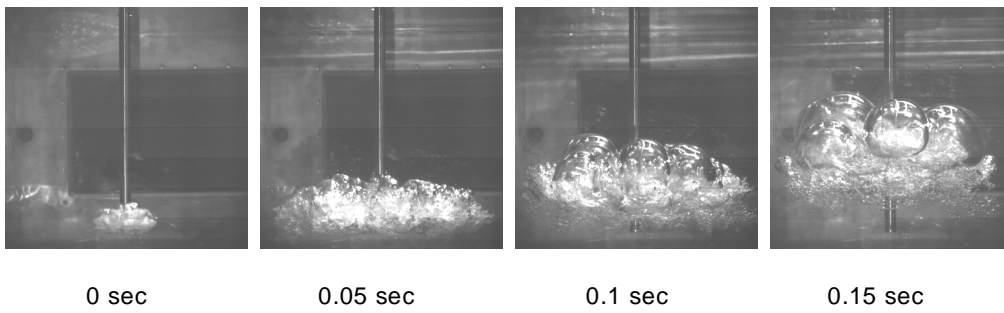


Fig. 15 Time history of air cloud formation

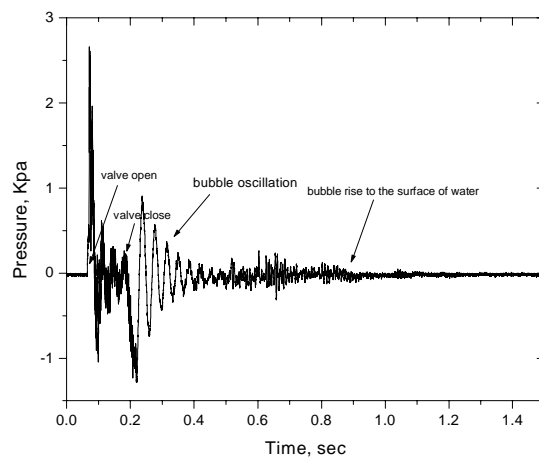


Fig. 16 Time history of pressure with air cloud oscillation

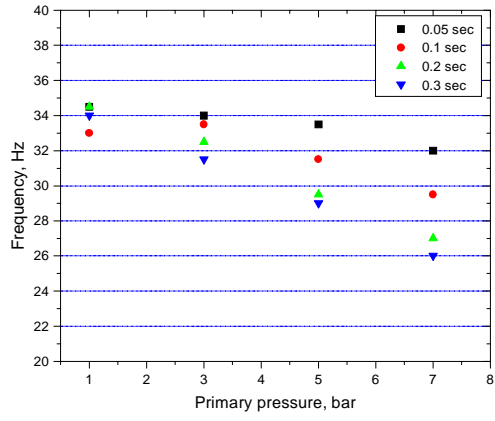


Fig. 17 Frequency variation with primary pressure nozzle with 8 hole

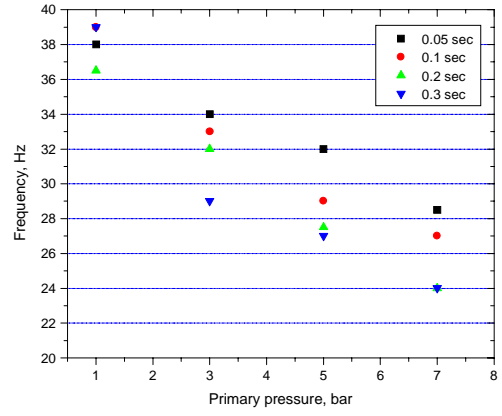


Fig. 18 Frequency variation with primary pressure nozzle with 24 hole